

First Observation of Quantum Interference in the Process $\phi \rightarrow K_S K_L \rightarrow \pi^+ \pi^- \pi^+ \pi^-$: a Test of Quantum Mechanics and CPT Symmetry

The KLOE Collaboration

F. Ambrosino^f, A. Antonelli^b, M. Antonelli^{b,1}, C. Bacci^ℓ,
P. Beltrame^c, G. Bencivenni^b, S. Bertolucci^b, C. Bini^j,
C. Bloise^b, S. Bocchetta^ℓ, V. Bocci^j, F. Bossi^b, D. Bowring^{b,n},
P. Branchini^ℓ, R. Caloi^j, P. Campana^b, G. Capon^b,
T. Capussela^f, F. Ceradini^ℓ, S. Chi^b, G. Chiefari^f,
P. Ciambrone^b, S. Conettiⁿ, E. De Lucia^b, A. De Santis^j,
P. De Simone^b, G. De Zorzi^j, S. Dell’Agnello^b, A. Denig^c,
A. Di Domenico^{j,2}, C. Di Donato^f, S. Di Falco^g, B. Di Micco^ℓ,
A. Doria^f, M. Dreucci^b, G. Felici^b, A. Ferrari^b, M. L. Ferrer^b,
G. Finocchiaro^b, S. Fiore^j, C. Forti^b, P. Franzini^j, C. Gatti^b,
P. Gauzzi^j, S. Giovannella^b, E. Gorini^d, E. Graziani^ℓ,
M. Incagli^g, W. Kluge^c, V. Kulikov^e, F. Lacava^j,
G. Lanfranchi^b, J. Lee-Franzini^{b,m}, D. Leone^c, M. Martini^b,
P. Massarotti^f, W. Mei^b, S. Meola^f, S. Miscetti^b,
M. Moulson^b, S. Müller^b, F. Murtas^b, M. Napolitano^f,
F. Nguyen^ℓ, M. Palutan^b, E. Pasqualucci^j, A. Passeri^ℓ,
V. Patera^{b,i}, F. Perfetto^f, L. Pontecorvo^j, M. Primavera^d,
P. Santangelo^b, E. Santovetti^k, G. Saracino^f, B. Sciascia^b,
A. Sciubba^{b,i}, F. Scuri^g, I. Sfiligoi^b, A. Sibidanov^{b,h},
T. Spadaro^b, M. Testa^{j,3}, L. Tortora^ℓ, P. Valente^j,
B. Valeriani^c, G. Venanzoni^b, S. Veneziano^j, A. Ventura^d,
R. Versaci^b, G. Xu^{b,a}

^aPermanent address: Institute of High Energy Physics of Academia Sinica, Beijing, China.

^bLaboratori Nazionali di Frascati dell’INFN, Frascati, Italy.

^cInstitut für Experimentelle Kernphysik, Universität Karlsruhe, Germany.

^dDipartimento di Fisica dell’Università e Sezione INFN, Lecce, Italy.

^e*Permanent address: Institute for Theoretical and Experimental Physics, Moscow, Russia.*

^f*Dipartimento di Scienze Fisiche dell'Università "Federico II" e Sezione INFN, Napoli, Italy*

^g*Dipartimento di Fisica dell'Università e Sezione INFN, Pisa, Italy.*

^h*Permanent address: Budker Institute of Nuclear Physics, Novosibirsk, Russia.*

ⁱ*Dipartimento di Energetica dell'Università "La Sapienza", Roma, Italy.*

^j*Dipartimento di Fisica dell'Università "La Sapienza" e Sezione INFN, Roma, Italy.*

^k*Dipartimento di Fisica dell'Università "Tor Vergata" e Sezione INFN, Roma, Italy.*

^l*Dipartimento di Fisica dell'Università "Roma Tre" e Sezione INFN, Roma, Italy.*

^m*Physics Department, State University of New York at Stony Brook, USA.*

ⁿ*Physics Department, University of Virginia, USA.*

¹ Corresponding author: Mario Antonelli, INFN - LNF, Casella postale 13, 00044 Frascati (Roma), Italy; tel. +39-06-94032728, e-mail mario.antonelli@lnf.infn.it

² Corresponding author: Antonio Di Domenico, Dipartimento di Fisica dell'Università "La Sapienza" e Sezione INFN, P.le A. Moro 2 00185 Roma, Italy; tel. +39-06-49914457, e-mail antonio.didomenico@roma1.infn.it

³ Corresponding author: Marianna Testa Dipartimento di Fisica dell'Università "La Sapienza" e Sezione INFN, P.le A. Moro 2 00185 Roma, Italy; tel. +39-06-49914614, e-mail marianna.testa@roma1.infn.it

Abstract

We present the first observation of quantum interference in the process $\phi \rightarrow K_S K_L \rightarrow \pi^+ \pi^- \pi^+ \pi^-$, using the KLOE detector at the Frascati e^+e^- collider DAΦNE. From about 5×10^4 neutral kaon pairs both decaying to $\pi^+ \pi^-$ pairs we obtain the distribution of Δt , the difference between the two kaon decay times, which allows testing the validity of quantum mechanics and CPT invariance: no violation of either is observed. New or improved limits on coherence loss and CPT violation are presented.

1 Introduction

A ϕ -factory provides unique opportunities for testing quantum mechanics (QM) and CPT symmetry. In the decay $\phi \rightarrow K^0 \bar{K}^0$, the neutral kaon pair is produced in a $J^{PC} = 1^{--}$ state:

$$\begin{aligned}
|i\rangle &= \frac{1}{\sqrt{2}} \left(|K^0, \mathbf{p}\rangle |\bar{K}^0, -\mathbf{p}\rangle - |\bar{K}^0, \mathbf{p}\rangle |K^0, -\mathbf{p}\rangle \right) \\
&= \frac{N}{\sqrt{2}} \left(|K_S, \mathbf{p}\rangle |K_L, -\mathbf{p}\rangle - |K_L, \mathbf{p}\rangle |K_S, -\mathbf{p}\rangle \right)
\end{aligned} \tag{1}$$

where \mathbf{p} is the kaon momentum in the ϕ meson rest frame, and $N = (1 + |\epsilon|^2)/(1 - \epsilon^2)$. Since $1 - N \ll 1$ we will set $N = 1$ in the following without any loss of generality. The decay intensity for the process $\phi \rightarrow (2 \text{ neutral kaons}) \rightarrow \pi^+ \pi^-$, $\pi^+ \pi^-$ is then given by [1]:

$$\begin{aligned}
I(t_1, t_2) &= \frac{1}{2} \left| \langle \pi^+ \pi^- | K_S \rangle \right|^4 |\eta_{+-}|^2 \left(e^{-\Gamma_L t_1 - \Gamma_S t_2} + e^{-\Gamma_S t_1 - \Gamma_L t_2} \right. \\
&\quad \left. - 2e^{-(\Gamma_S + \Gamma_L)(t_1 + t_2)/2} \cos(\Delta m(t_1 - t_2)) \right)
\end{aligned} \tag{2}$$

where t_i are the proper times of the two kaon decays, Γ_S and Γ_L are the decay widths of K_S and K_L , $\Delta m = m_L - m_S$ is their mass difference and $\eta_{+-} = \langle \pi^+ \pi^- | K_L \rangle / \langle \pi^+ \pi^- | K_S \rangle = |\eta_{+-}| e^{i\phi_{+-}}$. The two kaons cannot decay into the same final state at the same time, even though the two decays are space-like separated events. Correlations of this type in QM were first pointed out by Einstein, Podolsky, and Rosen (EPR) [2].

While it is not obvious what a deviation from QM might be, the assumption that coherence is lost during the states time evolution does violate QM. One can therefore introduce a decoherence parameter ζ [3], simply multiplying the interference term in Eq. (2) by a factor of $(1 - \zeta)$. The meaning and value of ζ depends on the basis in which the initial state (1) is written [4]. Eq. (2) is modified as follows:

$$\begin{aligned}
I(t_1, t_2; \zeta_{SL}) &= \frac{1}{2} \left| \langle \pi^+ \pi^- | K_S \rangle \right|^4 |\eta_{+-}|^2 \left(e^{-\Gamma_L t_1 - \Gamma_S t_2} + e^{-\Gamma_S t_1 - \Gamma_L t_2} \right. \\
&\quad \left. - 2(1 - \zeta_{SL}) e^{-(\Gamma_S + \Gamma_L)(t_1 + t_2)/2} \cos(\Delta m(t_1 - t_2)) \right)
\end{aligned} \tag{3}$$

in the K_S - K_L basis, and:

$$\begin{aligned}
I(t_1, t_2; \zeta_{0\bar{0}}) &= \frac{1}{2} \left| \langle \pi^+ \pi^- | K_S \rangle \right|^4 |\eta_{+-}|^2 \left(e^{-\Gamma_L t_1 - \Gamma_S t_2} + e^{-\Gamma_S t_1 - \Gamma_L t_2} \right. \\
&\quad - 2e^{-(\Gamma_S + \Gamma_L)(t_1 + t_2)/2} \cos(\Delta m(t_1 - t_2)) \\
&\quad + \frac{\zeta_{0\bar{0}}}{2} \left(-e^{-\Gamma_L t_1 - \Gamma_S t_2} - e^{-\Gamma_S t_1 - \Gamma_L t_2} \right. \\
&\quad \left. \left. + 2e^{-(\Gamma_S + \Gamma_L)(t_1 + t_2)/2} (\cos(\Delta m(t_1 - t_2)) - \cos(\Delta m(t_1 + t_2))) \right) \right) \\
&\quad + \frac{1}{2} \frac{\zeta_{0\bar{0}}}{|\eta_{+-}|^2} e^{-\Gamma_S(t_1 + t_2)} \quad \text{to the lowest order in } |\eta_{+-}|
\end{aligned} \tag{4}$$

in the K^0 - \bar{K}^0 basis.

Another phenomenological model [5] introduces decoherence via a dissipative term in the Liouville-von Neumann equation for the density matrix of the state

and predicts decoherence to become stronger with increasing distance between the two kaons. This model introduces a parameter λ , related to the decoherence parameter in the K_S - K_L basis by $\zeta_{SL} \simeq \lambda/\Gamma_S$.

In a hypothetical quantum gravity, space-time fluctuations at the Planck scale ($\sim 10^{-33}$ cm), might induce a pure state to become mixed [6]. This results in QM and CPT violation, changing therefore the decay time distribution of the K^0 - \bar{K}^0 pair from ϕ decays [7]. Three CPT - and QM-violating real parameters, with dimensions of mass, α , β , and γ , are introduced in [7]. α , β , and γ are guessed to be of $\mathcal{O}(m_K^2/M_P) \sim 2 \times 10^{-20}$ GeV [7,8], where $M_P = 1/\sqrt{G_N} = 1.22 \times 10^{19}$ GeV is the Planck mass. The conditions $\alpha = \gamma$ and $\beta = 0$ ensure complete positivity in this framework [9–11]. The decay intensity is (see Eq. (7.5) in Ref. [9] setting $\alpha = \gamma$ and $\beta = 0$):

$$I(t_1, t_2; \gamma) = \frac{1}{2} \left| \langle \pi^+ \pi^- | K_S \rangle \right|^4 |\eta_{+-}|^2 \left(\left(1 + \frac{\gamma}{\Delta\Gamma |\eta_{+-}|^2} \right) \left(e^{-\Gamma_L t_1 - \Gamma_S t_2} + e^{-\Gamma_S t_1 - \Gamma_L t_2} \right) - 2 \cos(\Delta m (t_1 - t_2)) e^{-(\Gamma_S + \Gamma_L)(t_1 + t_2)/2} - 2 \frac{\gamma}{\Delta\Gamma |\eta_{+-}|^2} e^{-\Gamma_S (t_1 + t_2)} \right) \quad (5)$$

It has been pointed out [12, 13] that in this context the initial state (1) may acquire a small C -even component:

$$|i\rangle = \frac{1}{\sqrt{2}} \left(|K^0, \mathbf{p}\rangle |\bar{K}^0, -\mathbf{p}\rangle - |\bar{K}^0, \mathbf{p}\rangle |K^0, -\mathbf{p}\rangle + \omega \left(|K^0, \mathbf{p}\rangle |\bar{K}^0, -\mathbf{p}\rangle + |\bar{K}^0, \mathbf{p}\rangle |K^0, -\mathbf{p}\rangle \right) \right) \quad (6)$$

where $\omega = |\omega|e^{i\Omega}$ is a complex parameter describing CPT violation, whose order of magnitude is expected to be at most $|\omega| \sim \sqrt{(m_K^2/M_P)/\Delta\Gamma} \sim 10^{-3}$, with $\Delta\Gamma = \Gamma_S - \Gamma_L$. The decay intensity is (see Eq.(3.3) in Ref. [13] setting $\alpha, \beta, \gamma = 0$):

$$I(t_1, t_2; \omega) = \frac{1}{2} \left| \langle \pi^+ \pi^- | K_S \rangle \right|^4 |\eta_{+-}|^2 \left(e^{-\Gamma_S t_1 - \Gamma_L t_2} + e^{-\Gamma_L t_1 - \Gamma_S t_2} - 2 \cos(\Delta m (t_1 - t_2)) e^{-(\Gamma_S + \Gamma_L)(t_1 + t_2)/2} + \frac{|\omega|^2}{|\eta_{+-}|^2} e^{-\Gamma_S (t_1 + t_2)} + 2 \frac{|\omega|}{|\eta_{+-}|} \left(\cos(\Delta m t_2 - \phi_{+-} + \Omega) e^{-\Gamma_S t_1 - (\Gamma_S + \Gamma_L)t_2/2} - \cos(\Delta m t_1 - \phi_{+-} + \Omega) e^{-\Gamma_S t_2 - (\Gamma_S + \Gamma_L)t_1/2} \right) \right) \quad (7)$$

The decoherence parameters ζ_{SL} and $\zeta_{0\bar{0}}$, have been found in the past to be compatible with zero, with uncertainties of 0.16 and 0.7, respectively, using CPLEAR data [4, 5, 14]. CPLEAR has also analyzed single neutral-kaon decays to measure the α , β , and γ parameters [15]. The values obtained for all three parameters are

compatible with zero, with uncertainties of 2.8×10^{-17} GeV, 2.3×10^{-19} GeV, and 2.5×10^{-21} GeV, respectively. The parameter ω has never been measured.

In the following, the improved KLOE measurements of the ζ_{SL} , $\zeta_{0\bar{0}}$, λ , γ , and ω parameters are presented. The analysis is based on data collected at DAΦNE in 2001–2002, corresponding to an integrated luminosity of $L \approx 380 \text{ pb}^{-1}$. DAΦNE, the Frascati ϕ factory, is an e^+e^- collider operated at a center of mass energy $W = M(\phi) \sim 1020$ MeV. Electrons and positrons collide in the horizontal plane at an angle of $\pi - 25$ mrad. ϕ -mesons are produced with approximately 12 MeV/c momentum toward the rings center, along the x -axis. The z -axis is taken as the bisectrix of the two beams, the y -axis being vertical.

2 The KLOE detector

The KLOE detector consists of a large, cylindrical drift chamber (DC), surrounded by a lead/scintillating-fiber electromagnetic calorimeter (EMC). A superconducting coil around the calorimeter provides a 0.52 T field. The drift chamber [16] is 4 m in diameter and 3.3 m in length. The momentum resolution is $\sigma_{p_\perp}/p_\perp \approx 0.4\%$. Two-track vertices are reconstructed with a spatial resolution of ~ 3 mm. The calorimeter [17] is divided into a barrel and two endcaps. It covers 98% of the solid angle. Cells close in time and space are grouped into calorimeter clusters. The energy and time resolutions for photons of energy E are $\sigma_E/E = 5.7\%/\sqrt{E}$ (GeV) and $\sigma_t = 57 \text{ ps}/\sqrt{E}$ (GeV) $\oplus 100$ ps, respectively. The KLOE trigger [18] uses calorimeter and chamber information. For this analysis, only the calorimeter signals are used. Two energy deposits above threshold ($E > 50$ MeV for the barrel and $E > 150$ MeV for the endcaps) are required.

Kaon regeneration in the beam pipe is a non negligible disturbance. The beam pipe is spherical around the interaction point, with a radius of 10 cm. The walls of the beam pipe, 500 μm thick, are made of a 62%-beryllium/38%-aluminum alloy (AlBeMet®162). A beryllium cylindrical tube of 4.4 cm radius and 50 μm thick, coaxial with the beam, provides electrical continuity.

We only use runs satisfying basic quality criteria. For each run we determine the average collision conditions: $\mathbf{p} = \mathbf{p}_{e^+} + \mathbf{p}_{e^-} = \mathbf{p}_\phi$, the center of mass energy W , the beam bunch dimensions, the collision point \mathbf{r}_C and angle. This is done using Bhabha scattering events. We then require $|p_{y,z}| < 3$ MeV, $|W - 1020| < 5$ MeV. The collision point must satisfy $|x_C| < 3$ cm, $|y_C| < 3$ cm, and $|z_C| < 5$ cm. The rms spread of the luminous region must satisfy $\sigma_x < 3$ cm and $\sigma_z < 3$ cm. A small number of runs were rejected because of improper trigger operation. Each run used in the analysis is simulated with the KLOE Monte Carlo (MC) simulation program, GEANFI [19], using values of relevant machine parameters such as W and \mathbf{p}_ϕ determined as mentioned above. Machine background obtained from data is superimposed on MC events on a run-by-run basis. For $K_S K_L \rightarrow \pi^+ \pi^- \pi^+ \pi^-$ events, the number of simulated events is 10 times that expected on the basis of the integrated luminosity. For all other processes, the effective statistics of the

simulated sample and of the data sample are approximately equal. The effects of initial- and final-state radiation are included in the simulation. Final-state radiation in K_S and K_L decays is treated as discussed in Ref. [20].

3 Analysis

3.1 Event selection

Events are selected on the basis of two identified neutral kaons from ϕ decay, in turn decaying into $\pi^+\pi^-$ pairs. Since we cannot tell whether $\pi^+\pi^-$ decays near the interaction point (IP) are from a K_S or a K_L , we try to ensure that the same criteria are used for all decays. In the following we call K_1 (K_2) the decay closest to (farthest from) the ϕ production point.

We first require a K_1 vertex with two tracks of opposite curvature within a fiducial volume with $r < 10$ cm and $|z| < 20$ cm centered at the nominal collision point \mathbf{r}_C , determined as discussed above. We also require that the two tracks satisfy $|m_{\pi^+\pi^-} - m_K| < 5$ MeV and $|p_{\pi^+\pi^-} - p_K| < 10$ MeV/ c , where p_K is calculated from the kinematics of $\phi \rightarrow K_S K_L$. $m_{\pi^+\pi^-}$ and $p_{\pi^+\pi^-}$ are respectively the invariant mass and the momentum of the $\pi^+\pi^-$ pair.

In order to search for a second $\pi^+\pi^-$ kaon decay (K_2), all relevant tracks in the chamber—after removal of those originating from the decay already identified—are extrapolated to their points of closest approach to the K_2 path computed from kinematics and \mathbf{x}_C . For each track candidate we compute d , the distance of closest approach to the K_2 path. For each charge we take the tracks with smallest value of d as the K_2 decay pions. We then determine the two track vertex and require that $|m_{\pi^+\pi^-} - m_K| < 5$ MeV and $|p_{\pi^+\pi^-} - p_K| < 10$ MeV/ c . We also require $-50 < E_{\text{miss}}^2 - p_{\text{miss}}^2 < 10$ MeV² and $\sqrt{E_{\text{miss}}^2 + p_{\text{miss}}^2} < 10$ MeV, where p_{miss} and E_{miss} are the missing momentum and energy computed assuming $K_2 \rightarrow \pi^+\pi^-$.

More accurate values for the $K_{1,2}$ vertex positions, $\bar{\mathbf{r}}_{1,2}$ and the collision point, $\bar{\mathbf{r}}_C$, are obtained from a kinematical fit. The fit makes use of the constraint from the K_1 and K_2 directions $\mathbf{n}_{1,2}$ defined by:

$$\mathbf{n}_{1,2} = \frac{(\mathbf{p}_+ + \mathbf{p}_-)_{1,2} - (\mathbf{p}_+ + \mathbf{p}_-)_{2,1} + \mathbf{p}_\phi}{|(\mathbf{p}_+ + \mathbf{p}_-)_{1,2} - (\mathbf{p}_+ + \mathbf{p}_-)_{2,1} + \mathbf{p}_\phi|}.$$

We then have

$$\bar{\mathbf{r}}_i = \bar{\mathbf{r}}_C + l_i \mathbf{n}_i, \quad i = 1, 2$$

and solve for $\bar{\mathbf{r}}_C$ and $l_{1,2}$ by maximizing the likelihood

$$\ln L = \sum_{i=1,2} \ln P_i(\mathbf{r}_i, \bar{\mathbf{r}}_C + l_i \mathbf{n}_i) + \ln P_C(\mathbf{r}_C, \bar{\mathbf{r}}_C),$$

where P_i and P_C are the probability density functions for \mathbf{r}_i and \mathbf{r}_C , respectively, as obtained from MC. The value of $l_{1,2}$ has been kept positive in the maximization.

The minimum of $-\ln L$ is shown in Fig. 1 for data and MC. In order to maximize

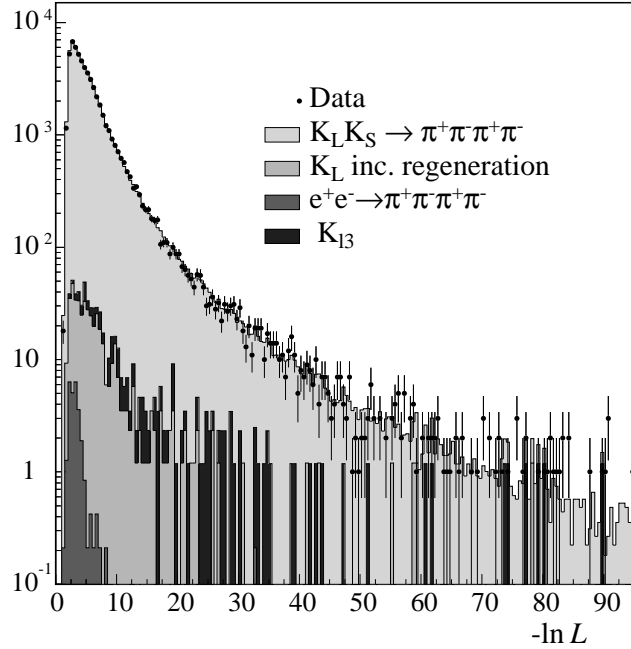


Fig. 1. Distribution of the minimum of $-\ln L$ of the kinematic fit for data and Monte Carlo for different decay channels.

signal efficiency, improve Δt resolution, and minimize incoherent regeneration background, as a final selection requirement we retain events with $-\ln L < 7.5$.

The time difference between $K_1 \rightarrow \pi^+\pi^-$ and $K_2 \rightarrow \pi^+\pi^-$ is determined as $\Delta t = |t_1 - t_2|$, where the proper time is $t_i = l_i / (\beta_i \gamma_i)$ with $\beta_i \gamma_i = p_{K_i} / m_K$.

3.2 Determination of background

The selected $K_S K_L \rightarrow \pi^+\pi^-\pi^+\pi^-$ events have a contamination of $\sim 3.2\%$ for $\Delta t < 35\tau_S$ dominated by regeneration on the beam pipe. Semileptonic K_L decays amount to 0.2% as determined from MC. Direct four pion production, $e^+e^- \rightarrow \pi^+\pi^-\pi^+\pi^-$, gives a $\sim 0.3\%$ contamination at the IP with $\Delta t \sim 0$, the region most sensitive to coherence loss. This contribution is obtained from the sidebands: $10 \text{ MeV} < \sqrt{E_{\text{miss}}^2 + p_{\text{miss}}^2} < 20 \text{ MeV}$ and $|p_{\pi^+\pi^-} - p_K| > 1 \text{ MeV}$. Vertex positions, total energy $E_{4\pi}$, and total momentum $p_{4\pi}$ are used to distinguish between $e^+e^- \rightarrow \pi^+\pi^-\pi^+\pi^-$ events and semileptonic K_L decays near the IP. We find 27 ± 8 events, in agreement with the estimate of ~ 32 events from the cross section given in Ref. [21].

Incoherent (see Sec. 3.4) and coherent regeneration on the beam-pipe are included in the fit of the Δt distribution. The coherent regeneration amplitude, $\rho_{\text{coh}} = |\rho_{\text{coh}}|e^{i\phi_{\text{coh}}}$, is obtained from the time distribution for $K_L(\rightarrow K_S) \rightarrow \pi^+\pi^-$ decays after single K_L 's cross the beam pipe:

$$\begin{aligned}
I(t) &= \left| \langle \pi^+ \pi^- | K_L(t) + \rho_{\text{coh}} | K_S(t) \rangle \right|^2 \\
&= \left| \langle \pi^+ \pi^- | K_S \rangle \right|^2 \left(|\eta_{+-}|^2 e^{-\Gamma_L t} + |\rho_{\text{coh}}|^2 e^{-\Gamma_S t} \right. \\
&\quad \left. + 2 |\eta_{+-}| |\rho_{\text{coh}}| e^{-(\Gamma_S + \Gamma_L)t/2} \cos(\Delta m t + \phi_{\text{coh}} - \phi_{+-}) \right)
\end{aligned} \tag{8}$$

K_L 's are identified by the reconstruction of a $K_S \rightarrow \pi^+ \pi^-$ decay, using the same algorithm used for the measurement of the $K_L \rightarrow \pi^+ \pi^-$ branching ratio [22]. In addition we require $|p_{K_L} - p_{\pi^+ \pi^-}| < 5$ MeV and $|E_{\pi^+ \pi^-} - \sqrt{p_{K_L}^2 + m_K^2} + m_{\pi^+ \pi^-} - m_K| < 5$ MeV, where the K_L momentum, p_{K_L} , is obtained from the K_S direction and \mathbf{p}_ϕ and $E_{\pi^+ \pi^-}$ is the energy of the $\pi^+ \pi^-$ pair. These cuts are effective for the identification of $K_L \rightarrow \pi^+ \pi^-$ decays and coherent and incoherent $K_L \rightarrow K_S \rightarrow \pi^+ \pi^-$ regeneration processes with a negligible amount of background. Incoherent regeneration is rejected by requiring that the angle between \mathbf{p}_{K_L} and $\mathbf{p}_{\pi^+ \pi^-}$ be smaller than 0.04. The residual contamination is $\sim 3\%$, from the sidebands of the distribution in the above angle. Fitting the proper-decay-time distribution, Eq. (8), we obtain $|\rho_{\text{coh}}| = (6.5 \pm 2.2) \times 10^{-4}$ and $\phi_{\text{coh}} = (-1.05 \pm 0.25)$ rad. This result is stable against variations of the scattering angle cut and agrees with predictions [23]. Coherent regeneration in the inner pipe is negligible. Background due to production of C -even neutral kaon pairs in two photon processes or (f_0 , a_0) decays is also negligible [1, 24–26].

3.3 Determination of the detection efficiency

The overall detection efficiency is about 30%, and has contributions from the event reconstruction and event selection efficiencies. These efficiencies have been evaluated from MC. For the reconstruction efficiency, a correction obtained from data is applied. This correction is determined using an independent sample of $K_S K_L \rightarrow \pi^+ \pi^-, \pi \mu \nu$ decays. $\pi \mu \nu$ decays are identified by requiring $\sqrt{E_{\text{miss}}^2 + p_{\text{miss}}^2} > 10$ MeV, $|p_{\pm}^*| < 246$ MeV and $p_+^* + p_-^* < 367$ MeV, where p^* is the momentum of the decay secondary in the kaon rest-frame, calculated assuming the π mass hypothesis. We then compute the squared lepton mass $m_{l^-}^2$ ($m_{l^+}^2$) in the hypothesis $K \rightarrow \pi^+ \mu^- \bar{\nu}$ ($K \rightarrow \pi^- \mu^+ \nu$), and require: $150 \text{ MeV}^2 < m_{l^-}^2 + m_{l^+}^2 < 270 \text{ MeV}^2$. The distribution of the time difference $\Delta t = |t_1 - t_2|$ between the two kaon decays obtained for the $K_S K_L \rightarrow \pi^+ \pi^-, \pi \mu \nu$ sample is shown in Fig. 2, both for data and MC. The correction to the reconstruction efficiency from the MC is obtained from the data-MC ratio of the distributions in Fig. 2 and applied bin by bin as a function of Δt .

In order to take into account the Δt resolution when fitting, a smearing matrix has been constructed from MC by filling a two-dimensional histogram with the “true” and reconstructed values of Δt . The efficiency correction and the smearing matrix are then used in the fit procedure as explained in the following section.

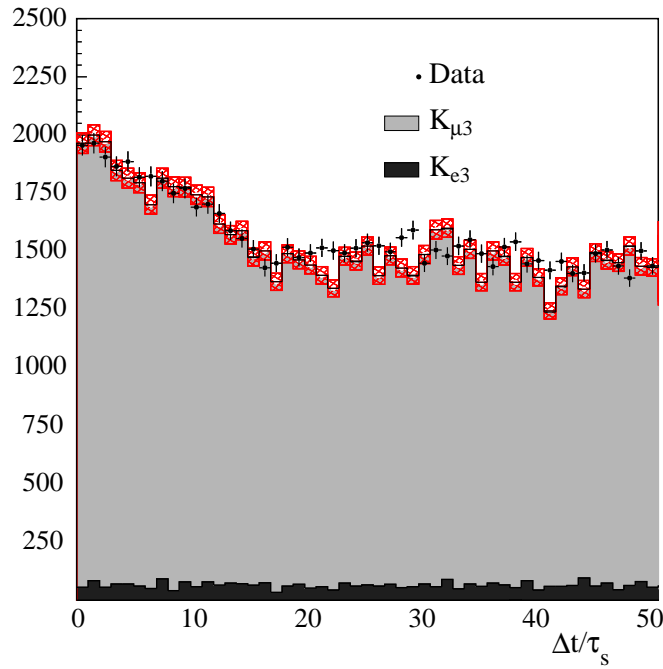


Fig. 2. Δt distribution for the $K_S K_L \rightarrow \pi^+ \pi^-, \pi \mu \nu$ control sample for data (black points) and Monte Carlo (solid histogram). The expected background contamination from $K_S K_L \rightarrow \pi^+ \pi^-, \pi e \nu$ is also shown. The hatched area represents the Monte Carlo statistical uncertainty.

3.4 Fit

We fit the observed Δt distribution between 0 and $35\tau_S$ in intervals of $\overline{\Delta t} = \tau_S$. The fitting function is obtained from the $I(t_1, t_2)$ distribution given in Eq. (2) including the QM violating parameter ζ , or the QM and CPT violating parameters γ and ω as discussed in Sec.1. To take coherent regeneration into account in Eq. (2), the time evolution of the single kaon is modified as follows:

$$|K_{S,L}(t_i)\rangle = |K_{S,L}(t_i)\rangle + \rho_{\text{coh}}|K_{L,S}(t_i)\rangle \quad (9)$$

where ρ_{coh} is evaluated as explained above. We then integrate $I(t_1, t_2)$ over the sum $t_1 + t_2$ for fixed $\Delta t = |t_1 - t_2|$, and over the bin-width of the data histogram:

$$I_j(\mathbf{q}) = \int_{(j-1)\overline{\Delta t}}^{j\overline{\Delta t}} d(\Delta t) \int_{\Delta t}^{\infty} I(t_1, t_2; \mathbf{q}) d(t_1 + t_2),$$

where \mathbf{q} is the vector of the QM- and CPT -violating parameters. Finally, the observed Δt distribution is fitted with the following function:

$$n_i = N \left(\sum_j s_{ij} \epsilon_j I_j(\mathbf{q}) \right) + N^{\text{reg}} I_i^{\text{reg}} + N_{4\pi} I_{4\pi, i} \quad (10)$$

where n_i is the expected number of events in the i^{th} bin of the histogram, s_{ij} is the smearing matrix, and ϵ_j is the efficiency. N , the number of $K_S K_L \rightarrow \pi^+ \pi^- \pi^+ \pi^-$ events, and N^{reg} , the number of events due to incoherent regeneration, are free parameters in the fit. The time distribution I_i^{reg} for the contribution from incoherent regeneration is evaluated from MC. The contribution from non-resonant $e^+ e^- \rightarrow \pi^+ \pi^- \pi^+ \pi^-$ events is treated in a similar manner, except for that $N_{4\pi}$ is fixed to the value determined as in Sec. 3.2, rather than left free in the fit. The fit is performed by minimizing the least squares function:

$$\chi^2 = \sum_{i=1}^n (N_i^{\text{data}} - n_i)^2 / (n_i + (n_i \delta\epsilon_i / \epsilon_i)^2) \quad (11)$$

where N_i^{data} is the number of events observed in the i^{th} bin and $\delta\epsilon_i$ is the error on the efficiency, including the correction. Using Eq. (10) with the QM- and CPT -violating parameters fixed to zero, Δm can be left as free parameter and evaluated. In this case, the fit gives

$$\Delta m = (5.61 \pm 0.33) \times 10^9 \text{ s}^{-1},$$

which is compatible with the more precise value given by the PDG [27]:

$$\Delta m = (5.290 \pm 0.015) \times 10^9 \text{ s}^{-1}.$$

For the determination of the QM- and CPT -violating parameters, Δm is fixed to the PDG value in all subsequent fits. As an example, the fit of the Δt distribution used to determine ζ_{SL} is shown in Fig. 3: the peak in the vicinity of $\Delta t \sim 17 \tau_S$ is due to coherent and incoherent regeneration on the spherical beam pipe.

3.5 Systematic uncertainties

As possible contributions to the systematic uncertainties on the QM- and CPT -violating parameters determined, we have considered the effects of data-MC discrepancies (in particular on the Δt resolution), dependences on cut values, and imperfect knowledge of backgrounds and other input parameters. The contributions from each source to the systematic uncertainty on each parameter determined are summarized in Tab. 1, and discussed in further detail in the following. Since the QM- and CPT -violating parameters are most sensitive to small values of Δt , particular attention has been devoted to the evaluation of systematic effects in that region. The dependence of the detection efficiency on Δt is mostly due to the cut on $-\ln L$ in the kinematic fit used to evaluate the vertex positions. We have varied the cut from 6.5 to 8.5, corresponding to a fractional variation in the efficiency of $\sim 5\%$. The corresponding changes in the final results are consistent with statistical fluctuations. For each physical parameter determined, we take the systematic error from this source to be half of the difference between the highest and lowest parameter values obtained as a result of this study. These contributions are listed in the first column of Tab. 1.

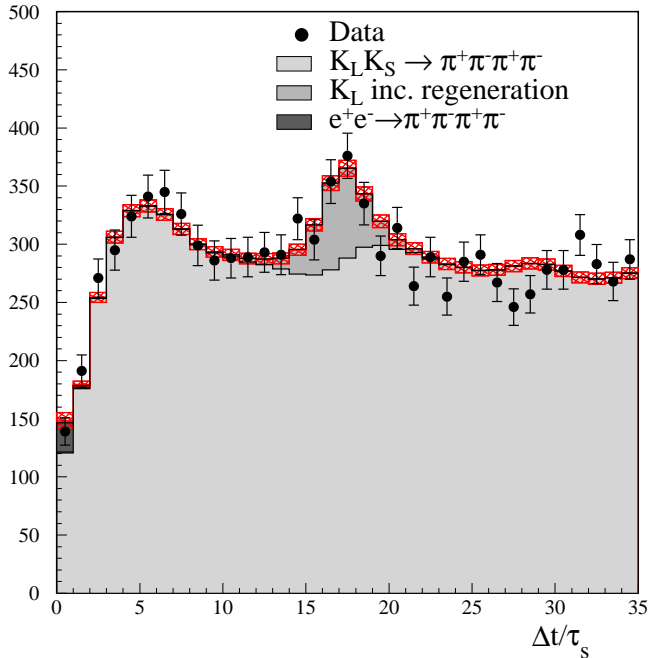


Fig. 3. Δt distribution from the fit used to determine ζ_{SL} . The black points with errors are data and the solid histogram is the fit result. The uncertainty arising from the efficiency correction is shown as the hatched area.

Table 1

Summary of systematic uncertainties

	Cut stability	Resolution	Inputs	Coherent reg.	$\pi^+\pi^-\pi^+\pi^-$ bckgnd
$\delta \zeta_{SL}$	0.007	0.002	0.001	0.001	0.020
$\delta \zeta_{00} \times 10^5$	0.03	0.01	0.01	-	0.11
$\delta \gamma \times 10^{21} \text{ GeV}$	0.4	0.2	0.1	0.3	1.3
$\delta \Re \omega \times 10^4$	0.8	0.1	0.1	0.3	1.4
$\delta \Im \omega \times 10^4$	0.4	0.4	0.2	0.3	0.1

The QM- and CPT -violating parameters depend also on the Δt resolution. We have checked the reliability of the MC simulation on a sample of events with $K_1=K_S$ $K_2=K_L$ by requiring $l_2 > 12$ cm and removing the $l_1 > 0$ cut. Fig. 4 shows the K_S proper-time distribution for data and MC. From the negative tail of the K_S proper-time distribution we obtain the experimental resolution. We fit the data and MC distributions to an exponential function convoluted with the resolution. We obtain an rms spread of $(1.152 \pm 0.020) \tau_S$ for data and $(1.1807 \pm 0.0036) \tau_S$ for MC, i.e., the data and MC resolutions agree to within 1.4 standard deviations. In addition, we obtain a K_S lifetime, $\tau_S = (0.9030 \pm 0.056) 10^{-10}$ s, in agreement with the world average value $(0.8958 \pm 0.0005) 10^{-10}$ s [27]. To estimate the resulting contributions to the systematic uncertainties on the QM- and CPT -violating parameters, the MC resolution is varied by $\pm 5\%$, about three times the statistical uncertainty of the check. For each parameter determined, we take the systematic

error from this source to be half of the difference between the highest and lowest values obtained. These contributions are listed in the second column of Tab. 1. The third column gives the contributions of uncertainties on the known values of Δm , Γ_L , Γ_S and η_{+-} , which have been propagated numerically.

Contributions to the systematic uncertainties due to limited knowledge on $|\rho_{\text{coh}}|$ and ϕ_{coh} have been evaluated by varying the parameter values within their errors and are listed in the fourth column of Tab. 1.

Finally the last column gives the contributions arising from the uncertainty on the level of background contamination from non-resonant $e^+e^- \rightarrow \pi^+\pi^-\pi^+\pi^-$ events, evaluated by varying the background parameter in the fits ($N_{4\pi}$ in Eq. (10)) within its error. Note, however, that these contributions are included in the statistical uncertainties, rather than in the systematic uncertainties, in the statement of the final results.

4 Results and conclusions

From the fit we obtain the decoherence parameter values:

$$\begin{aligned} \zeta_{SL} &= 0.018 \pm 0.040_{\text{stat}} \pm 0.007_{\text{syst}} & \chi^2/\text{dof} &= 29.7/32; \\ \zeta_{0\bar{0}} &= \left(0.10 \pm 0.21_{\text{stat}} \pm 0.04_{\text{syst}}\right) \times 10^{-5} & \chi^2/\text{dof} &= 29.6/32. \end{aligned}$$

which are consistent with $\zeta = 0$ and no QM modification. Using the Neyman procedure [28], we derive the upper limits $\zeta_{SL} < 0.098$ and $\zeta_{0\bar{0}} < 0.50 \times 10^{-5}$ at

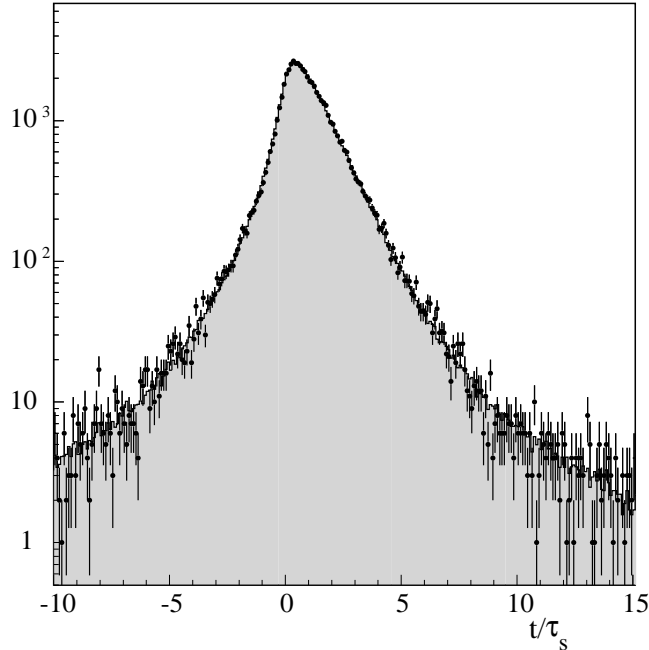


Fig. 4. Distribution of K_S proper-time distribution for data (black points) and Monte Carlo (solid histogram).

95% C.L. Since decoherence in the $K^0\bar{K}^0$ basis would result in the CP allowed $K_S K_S \rightarrow \pi^+ \pi^- \pi^+ \pi^-$ decays, Eq. 4, the value for ζ_{00} is naturally much smaller. In the model of Ref. [5], we find:

$$\lambda = (0.13 \pm 0.30_{\text{stat}} \pm 0.05_{\text{syst}}) \times 10^{-15} \text{ GeV}, \quad \lambda < 0.73 \times 10^{-15} \text{ GeV at 95\% C.L..}$$

All the above results are a considerable improvement on those obtained from CPLEAR data [4, 5]. We have measured the γ parameter:

$$\gamma = (1.3_{-2.4}^{+2.8} \pm 0.4) \times 10^{-21} \text{ GeV}$$

with $\chi^2/\text{dof} = 33/32$. From the above we find $\gamma < 6.4 \times 10^{-21} \text{ GeV}$ at 95 % C.L.. This result is competitive with that obtained by CPLEAR [15] using single kaon beams.

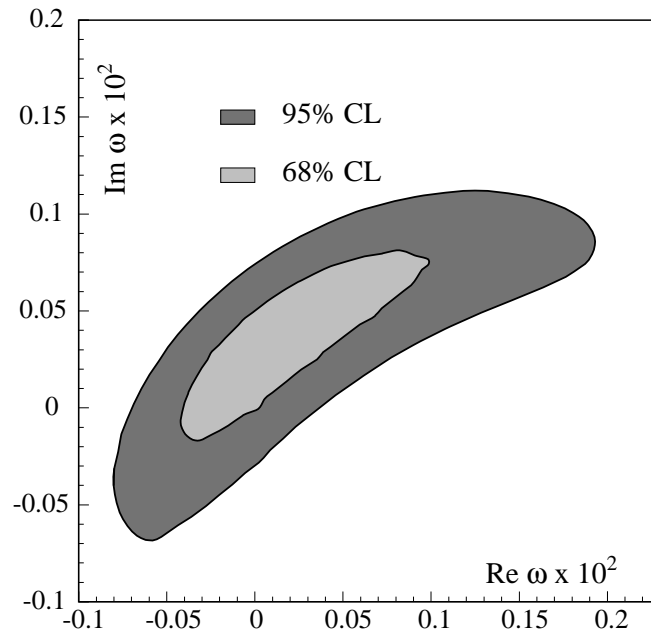


Fig. 5. Contour plot of $\Im \omega$ versus $\Re \omega$ at 68% and 95% C.L.

The complex parameter ω has been measured for the first time. The result is

$$\Re \omega = (1.1_{-5.3}^{+8.7} \pm 0.9) \times 10^{-4} \quad \Im \omega = (3.4_{-5.0}^{+4.8} \pm 0.6) \times 10^{-4}$$

with $\chi^2/\text{dof} = 29/31$. The correlation coefficient between $\Re \omega$ and $\Im \omega$ is 90%. Fig. 5 gives the 68% and 95% C.L. contours in the $\Im \omega$, $\Re \omega$ plane. The upper limit is $|\omega| < 2.1 \times 10^{-3}$ at 95% C.L.

We do not find any evidence for QM or CPT violation.

Acknowledgments

We thank the DAΦNE team for their efforts in maintaining low background running conditions and their collaboration during all data-taking. We want to thank our technical staff: G.F.Fortugno for his dedicated work to ensure an efficient operation of the KLOE Computing Center; M.Anelli for his continuous support to the gas system and the safety of the detector; A.Balla, M.Gatta, G.Corradi and G.Papalino for the maintenance of the electronics; M.Santoni, G.Paoluzzi and R.Rosellini for the general support to the detector; C.Piscitelli for his help during major maintenance periods. One of us, A.D.D., wishes to thank J. Bernabeu, R. A. Bertlmann, J. Ellis, M. Fidecaro, R. Floreanini, B. C. Hiesmayr, and N. Mavromatos, for private discussions. This work was supported in part by DOE grant DE-FG-02-97ER41027; by EURODAPHNE, contract FMRX-CT98-0169; by the German Federal Ministry of Education and Research (BMBF) contract 06-KA-957; by Graduiertenkolleg ‘H.E. Phys. and Part. Astrophys.’ of Deutsche Forschungsgemeinschaft, Contract No. GK 742; by INTAS, contracts 96-624, 99-37; by TARI, contract HPRI-CT-1999-00088.

References

- [1] I. Dunietyz, J. Hauser, J. L. Rosner, *Phys. Rev. D* **35**, (1987) 2166
- [2] A. Einstein, B. Podolsky, N. Rosen, *Phys. Rev.* **47**, (1934) 777
- [3] P.H. Eberhard, “Tests of Quantum Mechanics at a ϕ factory” in *The second Daφne handbook, Vol.I*, ed. L. Maiani, G. Pancheri, N. Paver, (1995) 99
- [4] R. A. Bertlmann, W. Grimus, B. C. Hiesmayr, *Phys. Rev. D* **60**, (1999) 114032
- [5] R. A. Bertlmann, K. Durstberger, B. C. Hiesmayr, *Phys. Rev. A* **68**, (2003) 012111
- [6] S. Hawking, *Commun. Math. Phys.* **87** (1982) 395
- [7] J. Ellis, J. S. Hagelin, D. V. Nanopoulos, M. Srednicki, *Nucl. Phys. B* **241**, (1984) 381
- [8] J. Ellis, J. L. Lopez, N. .E. Mavromatos, D. V. Nanopoulos, *Phys. Rev. D* **53**, (1996) 3846
- [9] P. Huet, M. Peskin, *Nucl. Phys. B* **434**, (1995) 3
- [10] F. Benatti, R. Floreanini, *Nucl. Phys. B* **511**, (1998) 550
- [11] F. Benatti, R. Floreanini, *Phys. Lett. B* **468**, (1999) 287
- [12] J. Bernabeu, N. Mavromatos, J. Papavassiliou, *Phys. Rev. Lett.* **92**, (2004) 131601
- [13] J. Bernabeu, N. Mavromatos, J. Papavassiliou, A. Waldron-Lauda, *Nucl. Phys. B* **744**, (2006) 180

- [14] A. Apostolakis *et al.*, CPLEAR Collaboration, *Phys. Lett. B* **422**, (1998) 339
- [15] R. Adler *et al.*, CPLEAR Collaboration, *Phys. Lett. B* **364**, (1995) 239
- [16] M. Adinolfi *et al.*, KLOE Collaboration, *Nucl. Instrum. Methods A* **488**, (2002) 51
- [17] M. Adinolfi *et al.*, KLOE Collaboration, *Nucl. Instrum. Methods A* **482**, (2002) 364
- [18] M. Adinolfi *et al.*, KLOE Collaboration, *Nucl. Instrum. Methods A* **492**, (2002) 134
- [19] F. Ambrosino *et al.*, KLOE Collaboration, *Nucl. Instrum. Methods A* **534**, (2004) 403
- [20] C. Gatti, *Eur. Phys. J. C* **45**, (2006) 417
- [21] R.R. Akhmetshin *et al.*, *Phys. Lett. B* **595**, (2004) 101
- [22] F. Ambrosino *et al.*, KLOE Collaboration, *Phys. Lett. B* **638**, (2006) 140
- [23] A. Di Domenico, *Nucl. Phys. B* **450**, (1995) 293
- [24] J. A. Oller, *Nucl. Phys. A* **714**, (2003) 161
- [25] N.N. Achasov, V. V. Gubin, *Phys. Rev. D* **64**, (2001) 094016
- [26] N.N. Achasov, V. V. Gubin, *Phys. Atom. Nucl.* **65**, (2002) 1887
- [27] W.-M. Yao *et al.*, Particle Data Group, *J. Phys. G* **33**, (2006) 1
- [28] G.J. Feldman, R. Cousins, *Phys. Rev. D* **57**, (1998) 3873